



# Pearls and Pitfalls in Imaging Bone Marrow in Pediatric Patients

Megha D. Patel, MD,<sup>\*</sup> James Brian, MD,<sup>†</sup> and Nancy A. Chauvin, MD<sup>†</sup>

Magnetic resonance is a noninvasive, nonionizing modality used in the detection and evaluation of marrow lesions, as well as surgical planning and treatment follow-up. Since the distribution of red and yellow marrow occurs in a predictable sequence according to age, understanding this sequence is essential in establishing an accurate and timely diagnosis. This article provides an overview of the normal appearance of bone marrow in healthy children as well as focal and diffuse marrow abnormalities. Imaging pitfalls unique to children and solutions to use in difficult cases will be described.

Semin Ultrasound CT MRI 41:472-487 © 2020 Elsevier Inc. All rights reserved.

## Introduction

Magnetic resonance (MR) imaging offers significant insight into the dynamic process of growth and maturation of the young skeleton. MR is an important modality in the detection and characterization of bone marrow lesions, evaluating marrow replacement processes, planning for biopsy or surgery, as well as playing an essential tool in treatment follow-up. As MR is complementary to histopathologic marrow assessment, there is increased reliance on MR to evaluate certain bone marrow diseases. The normal distribution of red and yellow marrow changes with age in a predictable sequence. Radiologists must be familiar with the MR appearance of normal bone marrow and be able to differentiate the expected age-related changes from pathology in order to make accurate, timely diagnoses. This article describes the appearance of normal bone marrow in the maturing skeleton, imaging pitfalls unique to children, troubleshooting solutions to use in difficult cases, and the MR characteristics of marrow lesions unique to growing children.

## Normal Bone Marrow

### Marrow Conversion and Appearance

Bone marrow is composed of hematopoietic, active “red” marrow as well as inactive, fatty “yellow” marrow. Hematopoietic marrow is high in water content (40%) and relatively low in fat content (40%) and contains approximately 20% of protein. Fatty marrow contains a much higher proportion of fat (80%) and less water (15%) and protein (5%).<sup>1</sup> In utero, hematopoiesis initially begins in the yolk sac and by the second trimester, extends to the liver and, to a lesser degree, the spleen. In the fourth fetal month, hematopoiesis appears within the bone marrow space. At birth, the marrow is entirely hematopoietic. During the first year of life, conversion from red to yellow marrow begins and continues until the adult pattern is reached by approximately 25 years of age.<sup>2</sup>

The MR appearance of marrow depends upon the age of the patient and the specific imaging sequence acquired. Conventional T1-weighted and T2-weighted spin echo (SE) (or other fluid-sensitive sequences) are the workhorse of MR imaging because tissue variation in T1 and T2 relaxation times allow for differentiation of normal red and yellow marrow. On T1-weighted imaging, the signal intensity of red marrow is considerably less than fatty marrow but typically higher than the adjacent muscles. The exception to this rule is in the neonatal period when a high percentage of cellularity causes normal marrow to appear isointense or hypointense relative to the muscles on T1-weighted images (Fig. 1). However, after the neonatal period, T1-weighted marrow signal that is lower than the adjacent normal muscle almost always

<sup>\*</sup>Department of Radiology, Penn State Milton S. Hershey Medical Center, Hershey, PA.

<sup>†</sup>Department of Radiology, Hershey Children's Hospital, Penn State Milton S. Hershey Medical Center, Hershey, PA.

Address reprint requests to Nancy A. Chauvin, MD, Department of Radiology, Hershey Children's Hospital, Penn State Milton S. Hershey Medical Center, 500 University Dr, Hershey, PA 17033 E-mail: [nchauvin@pennstatehealth.psu.edu](mailto:nchauvin@pennstatehealth.psu.edu)

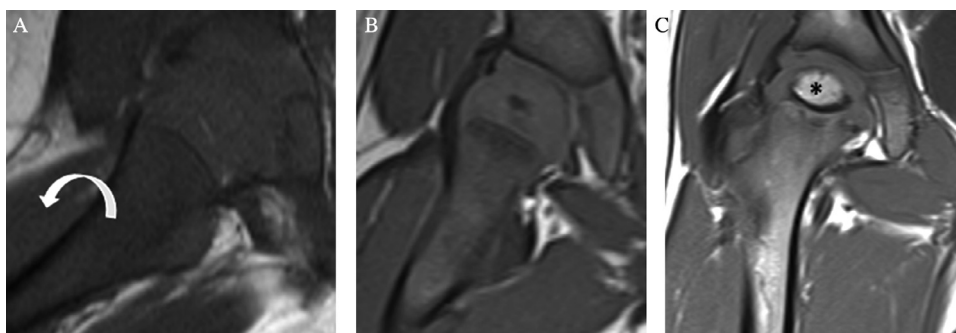


**Figure 1** Physiologic red marrow to yellow marrow conversion on coronal T1-weighted MR imaging of the right hip in 3 separate children. (A) A 3-week-old neonate demonstrates low signal intensity within marrow that is lower in signal intensity compared with the adjacent muscle (curved arrow). (B) A 9-month-old infant demonstrates early fatty marrow replacement with marrow signal intensity slightly higher than the adjacent muscle. (C) A 4-year-old child shows continued fatty marrow replacement. As expected, the epiphyses should contain fatty marrow throughout (\*) at this age as the proximal femoral epiphyseal ossification is radiographically apparent at approximately 6 months. After neonatal period, T1-weighted marrow signal lower than normal muscle almost always indicates pathology.



**Figure 2** Age-related changes of normal marrow in the knee on sagittal T2-weighted fat-saturated MR images in a (A) 15-month-old boy and (B) 6-year-old boy. The metaphyseal red marrow (\*) is more richly vascularized in the younger child and therefore is of higher signal intensity compared with the older child. On fluid-sensitive images, red marrow is isointense or slightly higher than that of adjacent normal muscle. Yellow marrow is isointense or slightly lower than that of subcutaneous fat.

indicates pathology.<sup>2,3</sup> On T2-weighted imaging, the signal intensity of red marrow is slightly brighter than the adjacent muscle and yellow marrow is isointense or slightly lower in signal than that of subcutaneous fat (Fig. 2).

The MR assessment of pediatric marrow is challenging due to age-related changes. Fortunately, red marrow to yellow marrow conversion occurs in a predictable pattern within the body as a whole as well as within each long bone. Marrow transformation begins in the periphery appendicular skeleton (fingers and toes) and progresses centrally (humeri and femora).<sup>3</sup> In each bone, conversion occurs first in the epiphyses, followed by the diaphysis and then the metaphyses, with the proximal metaphysis being the last to convert. Fatty marrow transformation in the epiphyses begins within 6 months of the radiologic appearance of the secondary ossification center (Fig. 3). Marrow reconversion (yellow to red), as seen in anemias and certain treatment-related changes, follows the

reverse pattern. Thus, the epiphyses are the last to reconvert to red marrow.<sup>3</sup>

Within the axial skeleton, the conversion of red to yellow marrow is much more gradual and continues throughout adulthood. With T1-weighted imaging of the spine, the signal intensity of the vertebral bodies is generally hypointense relative to the disks in infants less than 1 year of age. In children between the ages of 1 and 5 years, the vertebral bodies are relatively isointense to the disks. After 5 years of age, the bodies are hyperintense compared to the disks<sup>4</sup> (Fig. 4).

## Imaging Pitfalls Unique to Children

During the process of marrow conversion, the MR appearance of marrow in the healthy child may be a source of confusion.

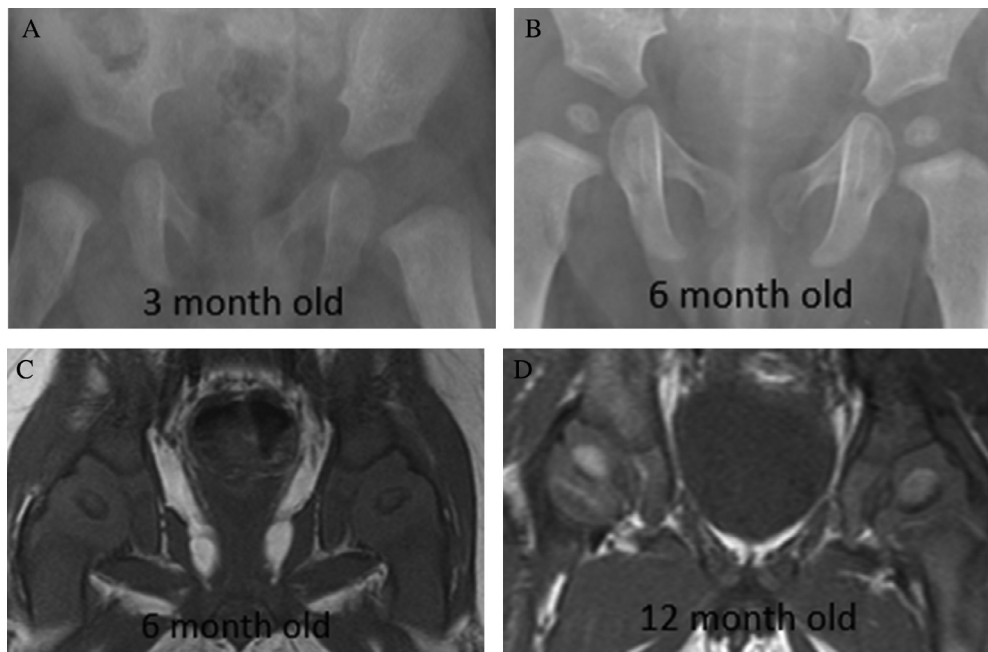


**Figure 3** Expected fatty marrow transformation of the epiphyses. (A) AP radiograph of a 3-month-old girl shows that the proximal femoral epiphyses are not yet ossified. (B) Early ossification centers are seen in a 6-month-old girl. Coronal T1-weighted MR images of the pelvis in a (C) 6-month-old girl and (D) 12-month-old girl demonstrate progressive fatty marrow transformation in the proximal femoral epiphysis. Conversion to fatty marrow begins within 6 months of the radiologic appearance of the secondary ossification center.

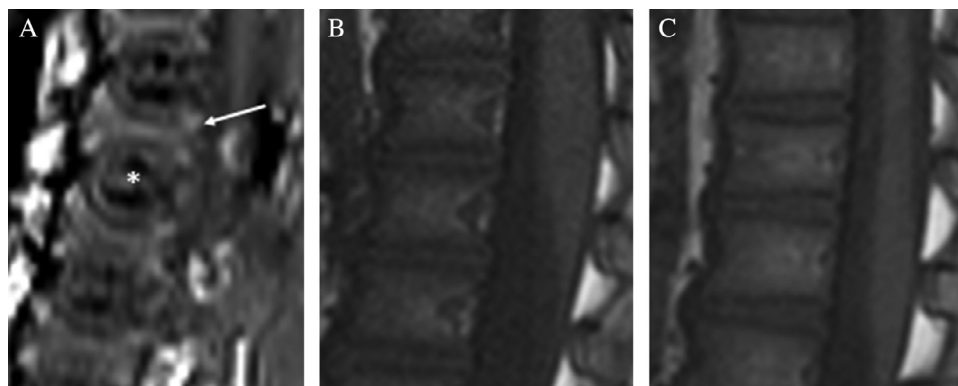


**Figure 4** Fatty marrow transformation of the axial skeleton on T1-weighted imaging. Sagittal T1-weighted MR images of the spine. (A) A 4-week-old boy. (B) A 3-year-old girl. (C) A 6-year-old girl. In infants less than 1 year of age, the vertebral bodies (\*) are generally hypointense relative to the intervertebral disks (arrow). Between the ages of 1 and 5 years, the vertebral bodies are isointense to the adjacent disk. In children older than 5 years, the vertebral bodies will appear hyperintense relative to the adjacent disks.

### Foci of Residual Red Marrow

Healthy children may demonstrate isolated foci of residual metaphyseal red marrow that have a “flame-shaped” appearance. These foci typically have a base adjacent to the physis and are characterized by straight margins. On T1-weighted sequences, the intensity of these foci should not be lower than the adjacent muscle (Fig. 5).<sup>3</sup> Within the epiphyses and apophyses, a hypointense rim can also be seen within the periphery on T1-weighted imaging. This pattern is due to the centrifugal pattern of marrow conversion in the secondary

ossification, which starts centrally and propagates toward the periphery.<sup>5</sup>

### Speckled Marrow of the Foot

Discrete foci of high signal intensity of fluid-sensitive sequences may be seen in the mid and hind foot bones of children who have altered weight bearing or who have been immobilized. These foci give rise to a “speckled” appearance of the marrow (Fig. 6). The etiology is controversial, but is thought to represent perivascular foci of red marrow. This finding

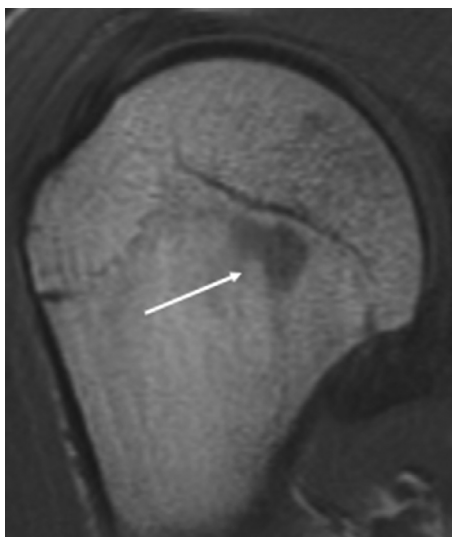


**Figure 5** Residual focus of red marrow. Coronal T1-weighted MR image of the proximal humerus in a 17-year-old boy demonstrates a hypointense region within the proximal humeral metaphysis (arrow). This focus is “flame-shaped” with a base parallel to the physis and vertical margins. On T1-weighted imaging, residual foci of red marrow should not be lower in signal than the adjacent muscle.

should not be mistaken for post-traumatic edema or stress-related changes.<sup>3,6</sup>

### Preossification Center

An important imaging pitfall to recognize is the “preossification center” of the developing epiphysis. The preossification center reflects the hypertrophic change that occurs in the cartilaginous epiphysis prior to the development of the secondary ossification center.<sup>7</sup> The preossification center occurs during the stage of bone development in which there is focal chondrocyte hypertrophy with breakdown of water-binding

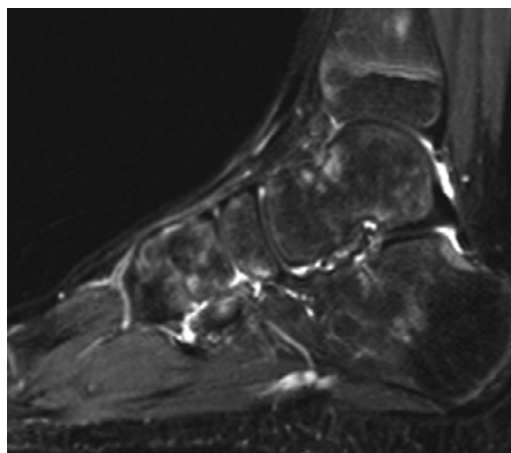


**Figure 6** Speckled marrow appearance of the foot. Sagittal STIR MR image of the mid and hindfoot in a 10-year-old boy shows multiple rounded foci of increased signal intensity throughout the visualized bones of the ankle and midfoot. The child had been immobilized for toe fractures. These foci are thought to be related to perivascular foci of red marrow and are not post-traumatic.

macromolecules of the matrix. The result is a focus of water signal which is typically globular in shape and well-circumscribed. On MR, the preossification center appears as a focal region of high signal intensity on fluid-sensitive sequences within the cartilaginous epiphysis and should not be mistaken for pathologic edema within the epiphyseal cartilage (Fig. 7).<sup>7</sup>

### Focal Periphyseal Edema

In adolescents approaching skeletal maturity, focal bone marrow edema can be seen centered in the physis, termed focal periphyseal edema (FOPE). On fluid sensitive MR sequences, FOPEs appear as focal areas of increased signal extending into the adjacent metaphysis and epiphysis (Fig. 8).<sup>8</sup> FOPEs are most commonly seen about the knee but may also be

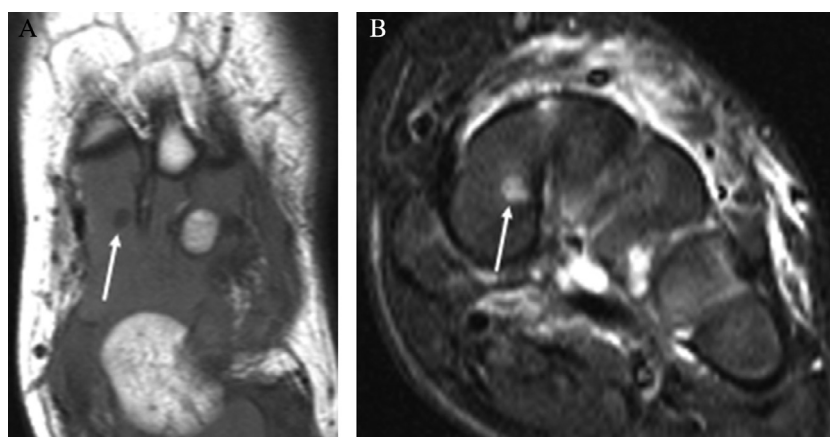


**Figure 7** Preossification center. A 1-year-old girl with foot swelling and fever. (A) T1-weighted MR footprint and (B) T2-weighted fat-saturated short axis MR images of the mid foot. Prior to the appearance of the secondary ossification center, there is an increase in free water and increased cellular volume leading to T2 prolongation and T1 shortening. This is seen in the medial cuneiform (arrow). This should not be mistaken for pathologic marrow edema. While the patient has edema within the soft tissues of the foot, there is no osteomyelitis.





**Figure 8** Focal periphyseal edema (FOPE). A 13-year-old girl with anterior knee pain. Coronal T2-weighted fat-saturated MR image of the knee demonstrates abnormal bone marrow edema within both the proximal tibial epiphysis and metaphysis, centered within the central aspect of the physis (arrow). A FOPE is thought to be a manifestation of normal skeletal maturation at physiologic physeal fusion and requires no invasive diagnostic procedure or imaging follow-up.

seen near other joints. Given the location and patient age, FOPEs are thought to represent signal changes related to the early stages of physiologic physeal closure. Importantly, this

finding should not be mistaken for an abnormality. FOPEs do not need to be confirmed with invasive diagnostic procedures and do not need imaging follow-up.<sup>8</sup>

## Imaging Techniques

### Chemical-Shift Imaging

Chemical-shift imaging may be useful in differentiating tumor vs normal marrow due to inherent difference in the resonance frequencies between water and lipid protons. With an appropriate echo time (eg, TE = 2.1ms for a 1.5T scanner), cellular lipid and water content influences the marrow signal intensity on opposed-phase imaging, resulting in a net cancellation of overall signal from voxels containing both lipid and water.<sup>9</sup> Red and fatty marrow both contain fat and water. Therefore, both types of marrow demonstrate signal drop out on opposed phase imaging. Conversely, tumor deposits in marrow do not demonstrate signal loss on opposed phase imaging because the vast majority of tumors do not contain fat<sup>10</sup> (Fig. 9). The presence of macroscopic regions of fat is also a reassuring finding indicating a benign process.

### Diffusion-Weighted Imaging

Diffusion-weighted imaging (DWI) quantitatively assesses the mobility of water molecules by allowing calculation of the apparent diffusion coefficient (ADC).<sup>10</sup> Tissues with higher cellular density with intact cell membranes; more complex fluid with hindrances; and cytotoxic edema all have

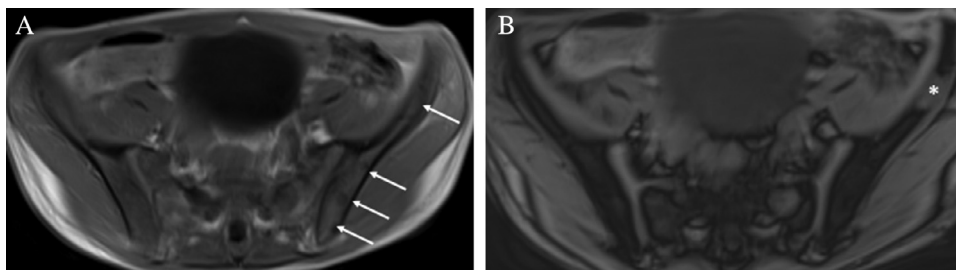


**Figure 9** Chemical shift imaging in neoplastic marrow. A 17-year-old girl with metastatic neuroblastoma, on therapy. (A) Axial in-phase and out-of-phase (B) MR imaging of the pelvis demonstrating multiple lesions within the left hemipelvis on in-phase imaging (arrows). On out-of-phase imaging, there is loss of signal drop out within the left iliac wing lesion (\*) in keeping with a marrow replacement process. The other lesions were not evident. The iliac wing lesion (\*) was confirmed to be tumor on MIBG imaging (not shown).

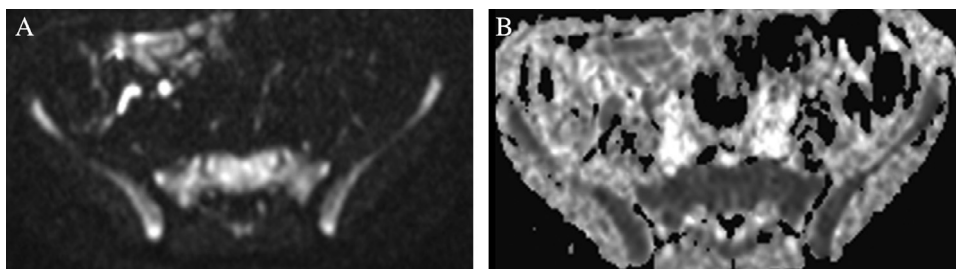


**Figure 10** Diffusion-weighted imaging in healthy marrow in a 5-year-old girl. Images obtained during MR urography for hydronephrosis. (A) Axial diffusion-weighted image of the pelvis, b = 800, demonstrates high signal throughout the pelvis with corresponding low signal on (B) ADC map compatible with diffusion restriction. This is due to highly cellular, hematopoietic marrow in the healthy young child.

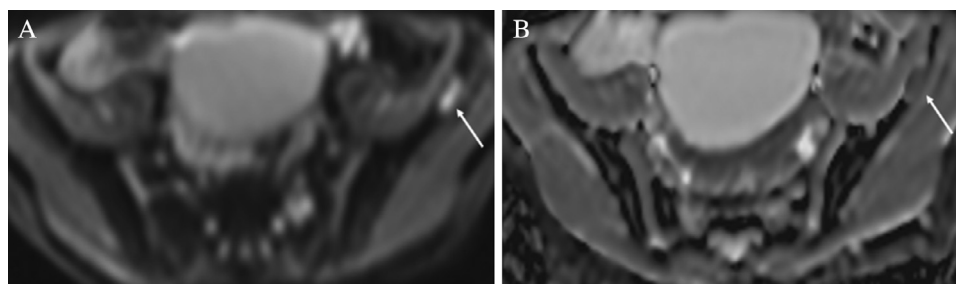


**Figure 11** Diffusion-weighted imaging in neoplastic marrow. A 17-year-old girl with metastatic neuroblastoma, on therapy (same patient as Fig. 9). (A) Axial diffusion-weighted image of the pelvis,  $b = 600$ , demonstrates focal high signal within the focal lesion within the left iliac wing (arrow) with corresponding low signal on (B) ADC map (arrow) compatible with diffusion restriction, compatible with active metastatic lesion which was confirmed to be tumor on MIBG imaging (not shown).

restricted water molecule mobility. Thus, highly cellular tumors, cytotoxic edema, abscess, and fibrosis demonstrate restricted diffusion.<sup>11</sup> It is important to note that in children, red marrow will restrict diffusion due to high percentage of cellularity (Fig. 10).<sup>12</sup> Ording Muller et al<sup>13</sup> demonstrated that restricted diffusion is a normal finding in the pelvic skeleton and lumbar spine in children as almost half of healthy children demonstrated an asymmetric distribution of restricted diffusion of the marrow. As such, the age of the patient and extent of red marrow should be considered when evaluating DWI in children.<sup>14</sup>

DWI imaging often provides little insight into further characterization of primary bone tumors over conventional MR imaging at the time of initial diagnosis. However, DWI may be a useful addition when assessing bone tumor response to therapy (Fig. 11). Changes in mean ADC values can be valuable in demonstrating necrosis and good response to treatment. Hayashida et al showed that when ADC values increased by approximately 95% in tumors, there was greater than 90% necrosis, indicative of a good response.<sup>15</sup>

### Whole Body MRI

Whole body MR imaging (WBMRI) is a useful modality to evaluate the extent and distribution of systemic and multifocal disease as well as for evaluating treatment response. WBMRI is particularly useful in children with known cancer predisposition syndromes who require repeated whole body imaging as it can be performed without ionizing radiation.<sup>12</sup> Technical developments such as the sliding table platform, software to enable seamless composite imaging and multi-channel coils have optimized imaging acquisition and quality. Radiologists use WBMRI to image both oncological and nononcologic diseases in children.<sup>16</sup> While there are no widely accepted imaging protocols, short tau inversion-recovery (STIR) imaging is widely used. Fast T2-weighted sequences such as single-shot turbo spin echo or half-Fourier acquisition single-shot turbo spine echo, and balanced steady-state free precession sequences that have a mix of T1- and T2-weighting are also commonly employed. For depiction of marrow lesions, T1-weighted fast spin-echo and/or gradient-echo imaging is often incorporated.<sup>12</sup> Dixon-based T1-weighted in and out of phase imaging has shown improved bone lesion detection in older children<sup>17</sup> and

provides for shorter scan times and higher signal to noise ratio. Coronal image acquisition reduces imaging time and is standard for most protocols. Axial and sagittal sequences are added based upon the study indication.

Additionally, some authors advocate for the use of DWI to enhance lesion depiction.<sup>16</sup> DWI with background body signal suppression (DWIBS) is commonly used for whole-body DWI. DWIBS using STIR achieves better fat suppression and less image distortion throughout the entire body than DWI using chemical shift selective pulse.<sup>16</sup> DWIBS imaging is often acquired in the axial plane during free-breathing and later reconstructed in coronal and sagittal planes.

WBMRI has been shown to be useful in the pediatric skeleton when assessing Langerhans cell histiocytosis, primary bone tumors (Ewing sarcoma), osseous metastases (small round blue cell tumors), multifocal osteonecrosis, cancer predisposition syndromes, chronic recurrent multifocal osteomyelitis, and multifocal osteomyelitis in very young children.<sup>12,18-20</sup>

### Intravenous Contrast

The use of intravenous gadolinium contrast should be judicious in children as it increases study cost, prolongs scan time (perhaps necessitating additional sedation medications) and subjects the child to potential adverse reaction (rarely allergic reaction, nephrogenic systemic fibrosis, possible effects of gadolinium deposits within the body). The clinical benefits of intravenous gadolinium should outweigh the theoretical risks if contrast is to be used in a pediatric patient.<sup>21</sup>

## Malignancies

### Aggressive Bone Lesions

#### Primary Osseous Sarcomas

Osteosarcoma and Ewing's sarcoma are the first and second most common primary bone tumor in childhood, respectively.<sup>22</sup> Both sarcomas have a male predominance and typically present in the second decade of life in children.<sup>23,24</sup> Ewing's sarcoma is a small round blue cell tumor with MR features that demonstrate bone marrow replacement characterized by a hypointense signal on T1-weighted imaging and

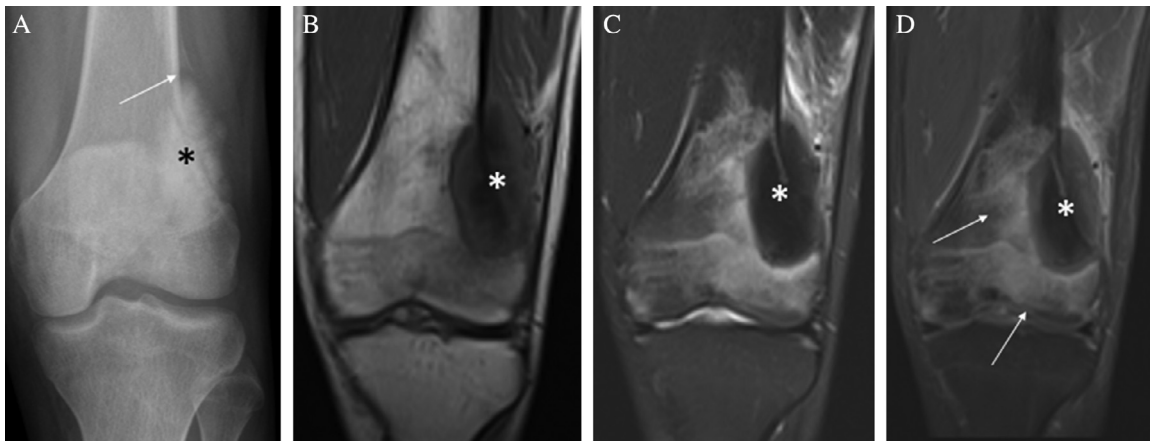


**Figure 12** Primary osseous sarcoma. A 16-year-old boy with distal left femur pain and swelling. (A) Frontal radiograph of the left knee demonstrates a mass within the lateral aspect of the distal femur with an osteoid matrix (\*) and aggressive periosteal reaction superiorly (arrow). On coronal T1-weighted (B), T2-weighted fat-saturated (C) and T1-weighted fat-saturated postcontrast images (D), the mass demonstrates diffusely low signal due to the osteoid matrix (\*). There is perilesional marrow edema with adjacent soft tissue edema which enhances after contrast (arrows). T1-weighted imaging best demonstrates the borders of the sarcoma.

hyperintense signal on T2-weighted imaging.<sup>25</sup> Ewing's sarcoma lesions are often associated with cortical destruction and a soft tissue mass.<sup>25,26</sup> Osteosarcoma is the most common malignant bone tumor seen in children.<sup>22</sup> It presents in children between the ages of 10 and 15 years<sup>23</sup> with a male predominance.<sup>22,23</sup> MR findings of osteosarcoma typically demonstrate low T1 and T2 signals which vary based on the degree of tumor mineralization (Fig. 12).<sup>1</sup> In the work-up of a primary osseous sarcoma, it is important to image the entire affected bone as the tumor can present with skip metastasis.<sup>27</sup>

### Lymphoma

Primary osseous lymphoma is rare in the pediatric population.<sup>28,29</sup> Pain is the most common presenting feature.<sup>14</sup> Bone marrow replacement in lymphoma is characterized by hypointense marrow signal on T1-weighted imaging, hyperintense marrow signal on T2-weighted imaging, and enhancement after contrast administration.<sup>1,30</sup> Lymphomatous involvement in the bone marrow is often focal and patchy rather than diffuse, contributing to frequent false negatives on bone marrow biopsy.<sup>9,14</sup> In addition to osseous involvement, lymphoma can be associated with a soft tissue mass on MR.<sup>30</sup>

### Metastatic Disease

Bone marrow metastases may be either focal or multifocal and most commonly affect the vascularized red marrow.<sup>1,2</sup> The most common primary tumors in the pediatric population with bone marrow metastases are neuroblastoma and rhabdomyosarcoma.<sup>2</sup> At diagnosis, bone marrow involvement is seen in 71% of neuroblastomas<sup>31</sup> and 6% of rhabdomyosarcomas.<sup>32</sup> Neuroblastomas and rhabdomyosarcomas can have diffuse bone marrow involvement, appearing similar to leukemia on MR. MR of metastatic lesions typically demonstrates a peripheral hyperintense rim ("halo sign") on

fluid sensitive sequences, representing fluid replacement from trabecular destruction.<sup>1</sup>

### Langerhans Cell Histiocytosis

Langerhans cell histiocytosis (LCH) is a rare disorder that results from an abnormal accumulation of a Langerhans cell within an organ system. In children, the disease typically occurs between the ages of 5 and 15 years, at an incidence rate of 4.6 cases per million per year.<sup>33</sup> LCH most commonly affects the skeletal system. In approximately 70% of LCH cases, the disease is limited to a single bone or a few bones. Long bone involvement is more common in children than adults. The femur, humerus, and tibia are often involved and lesions typically occur in the diaphysis or metaphysis. On conventional radiographs, lesions often appear lytic, expansile, and aggressive.<sup>34</sup> The skull is the most common flat bone involved, followed by the mandible, ribs, pelvis, and spine. The typical presentation is pain which may be associated with a soft tissue mass.<sup>14,35</sup>

MR of LCH demonstrates intramedullary lesions characterized by a hypointense signal on T1-weighted imaging with postcontrast enhancement and a hyperintense signal on fluid-sensitive sequences, with or without an extramedullary soft tissue component.<sup>1,14,35</sup> Early lesions can present with features of bone marrow edema, periosteal reaction, and endosteal scalloping, appearing similar to malignancy and osteomyelitis.<sup>35,36</sup> Therefore, diagnosis is confirmed with biopsy.<sup>14</sup> Treatment with chemotherapy will show an interval decrease in signal intensity on STIR imaging and decrease in contrast enhancement on T1 weighted imaging.<sup>37</sup> As lesions become chronic, they will appear more sclerotic from periosteal new bone formation.<sup>34</sup>

### Liquid Tumors

Acute leukemia is the most common pediatric malignancy with the acute lymphoblastic leukemia representing the most common subtype. There are 3 types of bone marrow patterns

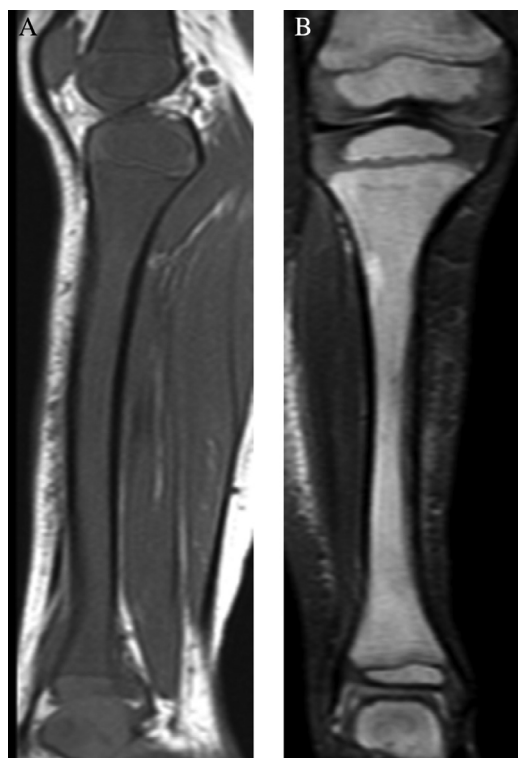


**Figure 13** Leukemia. A 3-year-old boy with bilateral leg pain. (A) Sagittal T1-weighted and (B) coronal STIR MR images of the right tibia demonstrate the marrow “flip-flop” sign. There is infiltration of the marrow as demonstrated by diffuse loss of the expected fatty marrow signal intensity on the T1-weighted image. On STIR, there is abnormal, increased signal intensity throughout the bones (reverse of what is expected). Of note, the distal femoral and proximal tibial epiphyses should be radiographically apparent by 3 months of age and therefore normal fatty conversion should occur before the age of 1 year.

in leukemia: diffuse, patchy, and focal.<sup>2,38</sup> Of these patterns, the diffuse type is the most common. The leukemic cells will replace the normal fatty marrow, resulting in a characteristic loss of bright T1-weighted fatty marrow signal and an

increase in the fluid sensitive signal intensity known as the “flip flop sign” (Fig. 13).<sup>1</sup>

Bone marrow necrosis and bone marrow infarction (osteonecrosis) can occur with acute lymphoblastic leukemia. In early disease, these 2 entities are indistinguishable on MR.<sup>39</sup> Postcontrast imaging of bone marrow necrosis will demonstrate peripheral enhancement of the affected marrow (Fig. 14).<sup>39</sup> Bone marrow infarction may demonstrate the classic “double line” sign on fluid sensitive imaging due to a combination of edema and necrosis.<sup>40</sup>

## Treatment-Related Marrow Changes

### Radiation Therapy

Radiation therapy and granulocyte colony stimulating factor are used in the treatment of pediatric skeletal neoplasms. Radiation is localized to the area of diseased bone to prevent the spread of tumor. Radiation therapy disrupts the normal distribution of red and yellow bone marrow. It destroys the vasculature structures, resulting in replacement of red marrow by yellow marrow.<sup>41</sup> Within the first 3 weeks of radiation therapy, the bone marrow demonstrates no change or a subtle increase in T2 signal intensity due to edema and necrosis.<sup>42</sup> Around 3 weeks post-therapy, bone marrow demonstrates a heterogeneous T1 signal intensity as red marrow is replaced by fatty marrow. As there is more fatty conversion, over time the T1 signal intensity appears homogeneous (Fig. 15).<sup>42</sup> Fatty conversion appears in the irradiated bone marrow as well as the adjacent bone marrow.<sup>43</sup>

The bone marrow can regenerate, depending upon the patient's age and radiation dose.<sup>43,44</sup> Fatty conversion has been shown to be reversible with radiation dosing of less than 30-40 Gy, but is irreversible with doses greater than 40 Gy.<sup>43,44</sup> Furthermore, the pediatric population is more likely to regenerate to normal bone marrow compared to older patients.<sup>44</sup> One complication of radiation therapy unique to the pediatric population is that radiation can impair growth at the physes (Fig. 16).<sup>45</sup> Childhood cancer survivors treated with pelvic radiation are at risk for development of slipped

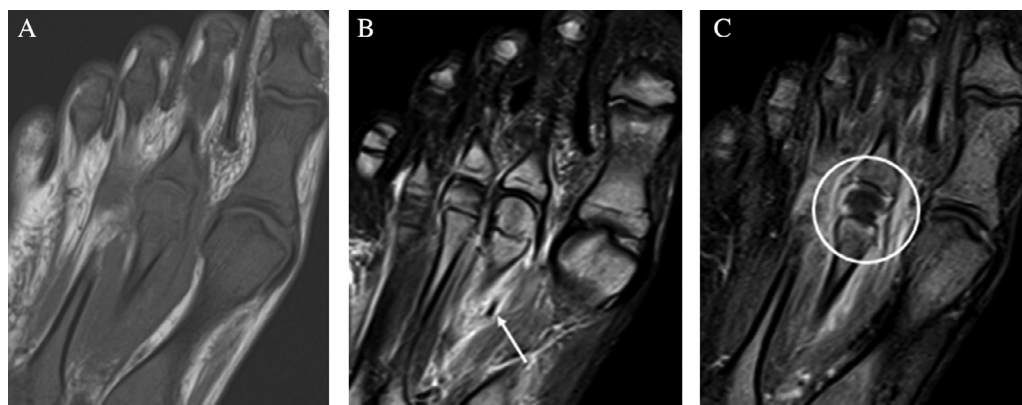


**Figure 14** Acute bone infarction in setting of newly diagnosed B-cell leukemia. A 14-year-old girl with fatigue, pallor, and toe pain. MR obtained to evaluate for osteomyelitis. (A) Footprint T1-weighted MR image of the forefoot demonstrates diffusely decreased marrow signal intensity with diffusely increased marrow signal on STIR (B) imaging consistent with a marrow replacement process. There is soft tissue edema seen along the mid to distal second metatarsal (arrow). (C) Footprint T1-weighted fat-saturated postcontrast MR image shows nonenhancement of the second metatarsal epiphysis, in keeping with bone infarction in the setting of leukemia. Her pain improved without antibiotics.



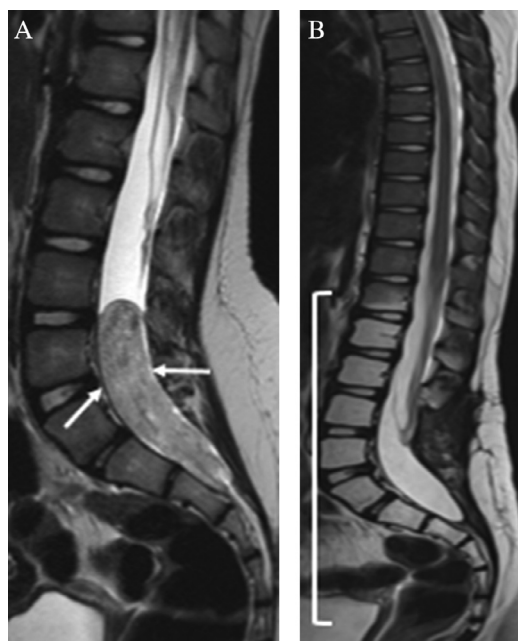


**Figure 15** Radiation therapy changes. A 12-year-old girl with myxopapillary ependymoma. (A) Sagittal T2-weighted MR image of the lumbosacral spine demonstrates a mass within the distal spinal canal (arrows). There is normal marrow signal of the vertebral bodies. (B) Follow-up sagittal T2-weighted MR image (1 year later) obtained after tumor resection, chemotherapy, and external beam radiation shows fatty marrow replacement of the lumbar and sacral spine vertebral bodies with a discrete transition between normal and abnormal, fatty marrow in the region of the radiation portal (bracket).

capital femoral epiphysis. This risk is increased with the use of recombinant growth hormone.<sup>46</sup>

### Marrow Stimulating Agents

Granulocyte colony-stimulating factor (G-CSF) is given as an adjunct to chemotherapy and radiation in order to enhance the bone marrow reversion. G-CSF decreases aplasia and activates the hematopoietic bone marrow by stimulating cell production.<sup>43</sup> MR characteristics of G-CSF-induced reversion occur in a diffuse pattern that can be difficult to differentiate from malignancy. On T1-weighted imaging, G-CSF-induced reversion demonstrates a low T1 signal intensity, which is nonspecific and can also occur with malignancy. However, the T1 signal should not be lower than the adjacent muscle. On T2-weighted imaging, hematopoietic reversion manifests as a low T2 signal intensity relative to fat (Fig. 17).<sup>47</sup> This process peaks approximately 2 weeks after the administration of the agent. In-phase/out-of-phase imaging is often used to assess fatty infiltrate that is present in marrow hyperplasia but rare in metastasis.

## Blood Dyscrasias

### Hemoglobinopathies

Anemia is a prevalent pediatric condition with a variety of etiologies.<sup>48</sup> Sickle cell anemia and beta thalassemia are



**Figure 16** Radiation therapy changes. A 13-year-old boy with history stage IV neuroblastoma (at age 4 years) which was treated with chemotherapy and total body irradiation. Sagittal T2-weighted fat-saturated MR image of the knee shows irregularity of the distal femoral and proximal tibial physes with high signal intensity metaphyseal tongues of cartilage (arrows) related to enchondral ossification disruption resulting from prior radiation induced damage of the normal metaphyseal vascularity.

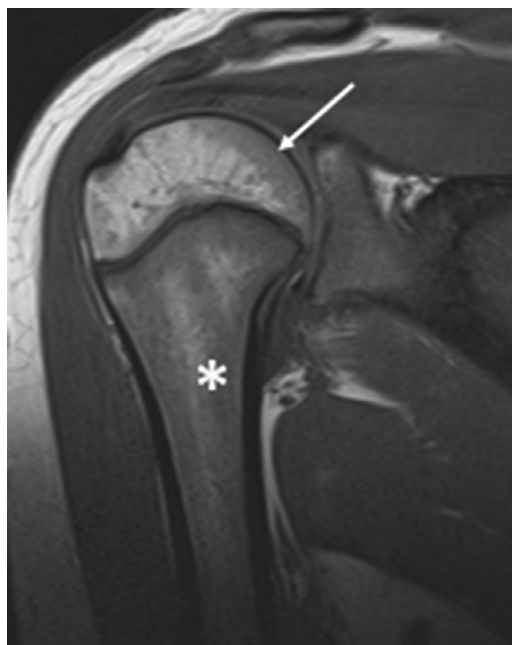


**Figure 17** Chemotherapy-related marrow change. A 17-year-old girl with history of lower extremity osteosarcoma, on chemotherapy and bone marrow stimulating agents. Reported right shoulder pain. Coronal T1-weighted image of the shoulder demonstrates changes of marrow reversion/stimulation with low T1-weighted signal within the proximal humeral shaft (\*). In addition, there is a halo of low signal within the peripheral aspect of the epiphysis (arrow). In marrow reversion, the epiphyses are the last to reconvert.

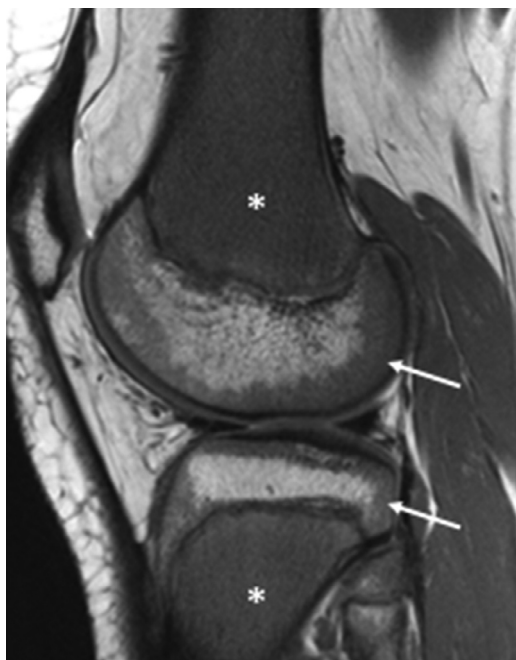


**Figure 18** Red marrow hyperplasia. A 17-year-old boy with sickle cell disease. Sagittal T1-weighted MR image of the knee demonstrates diffuse, homogeneous hematopoietic marrow within the metaphyses (\*) with a halo of hematopoietic marrow within the periphery of the epiphyses (arrows). Marrow reconversion occurs in the reverse pattern of normal fatty marrow conversion. The epiphyses are the last to revert.

congenital forms of anemia caused by genetic defects of the beta globin gene on chromosome 11. Both conditions result in severe anemia, either as the result of shortened red blood cell life span (sickle cell anemia) or ineffective hemoglobin

synthesis (beta thalassemia). The severity of clinical presentation varies depending on the nature of the chromosomal abnormality.<sup>49,50</sup> Patients afflicted by these hemoglobinopathies often require imaging as part of their treatment and care.

The profound anemia of sickle cell disease and beta thalassemia stimulates the intramedullary bone marrow to produce red blood cells. This lifelong chronic hematopoietic stress can lead to an arrest of the normal conversion of yellow marrow or a persistence of red marrow.<sup>51,52</sup> As previously described, the reconversion of yellow marrow to red marrow follow the reverse order of the typical marrow conversion. Reconversion occurs first in the vertebra and pelvis followed by the long bones. Long bone marrow reconversion occurs initially in the proximal metaphyses, then the distal metaphyses and finally the diaphyses. Epiphyseal and/or apophyseal reconversion is rarely seen in the setting of severe anemia (Fig. 18).<sup>53</sup> Similarly, patients experiencing lifelong hematopoietic stress will demonstrate persistence of red marrow in the vertebra and flat bones of the axial skeleton as well as the metaphyses and diaphyses of their larger long bones.<sup>51</sup> With MR, the appearance of nonconverted and reconverted red bone marrow can mimic neoplastic replacement bone marrow. In distinguishing between the two entities, it is helpful to note that red marrow will follow the aforementioned symmetric orderly pattern and will not demonstrate cortical breakthrough, soft tissue extension, or the degree of enhancement expected with infiltrative neoplastic lesions. Also, hematopoietic marrow also does not have the same amount of increased T2 signal expected from invasive bone lesions.<sup>2</sup>

Hyperplasia of red marrow can also result in expansion of the marrow cavity, a finding that can be seen on plain

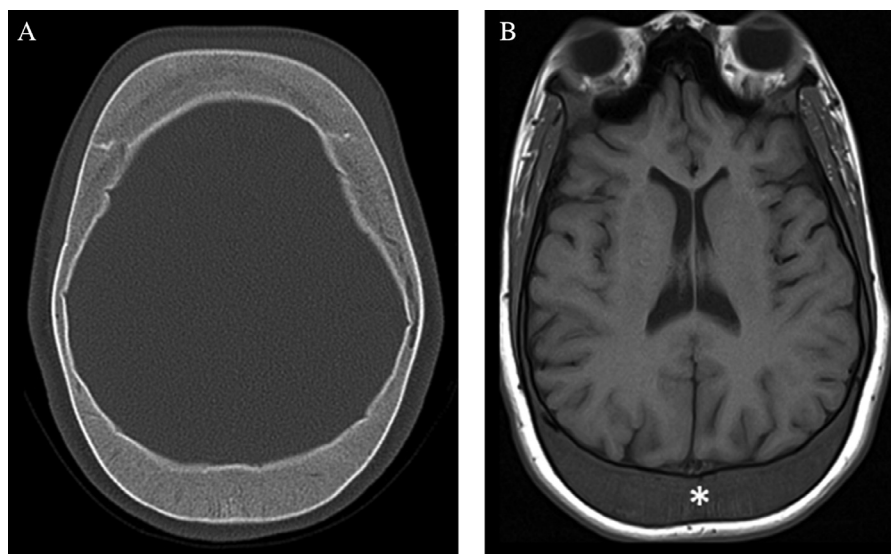


**Figure 19** Sickle cell disease. A 17-year-old girl with sickle cell disease and headache. Axial (A) noncontrast CT of the head in bone windows and (B) T1-weighted MR images of the brain show marrow expansion with widening of the calvarial diploic spaces due to red marrow hyperplasia (\*). Note the low T1-weighted signal of red marrow relative to the hyperintense adjacent subcutaneous fat.

radiographs as well as CT and MR. The typical example of marrow expansion is the widening of the calvarial diploic space seen on cross sectional head imaging (Fig. 19).<sup>54</sup>

## Myelofibrosis

In children, myelofibrosis is rare and may be idiopathic, related to malignancy, or secondary to treatment with radiation or chemotherapeutic agents.<sup>55,56</sup> Fibrous replacement of marrow will result in low signal intensity on T1- and T2-weighted images. Variability in MR signal can result from residual marrow cellularity or fat.<sup>2</sup>

## Nutritional and Metabolic Conditions

### Scurvy

Scurvy is a nutritional deficiency that results from an inadequate intake of a vitamin C (ascorbic acid). Although rare in the United States, scurvy occurs in patients with severely unbalanced diets. In the pediatric population, scurvy is diagnosed most commonly in children with food avoidant disorders (such in autism)<sup>57</sup> and patients with overall poor oral intake.<sup>58</sup> On MR, scurvy initially affects the metaphyses (sites of greatest bone turnover) and demonstrates decreased T1 and increased T2 signal intensities within the marrow that may be associated with large subperiosteal fluid collections<sup>57-59</sup> (Fig. 20). These nonspecific findings

can also be seen with osteomyelitis, subperiosteal abscess, anemia or leukemia, so correlation with laboratory values and clinical scenario is critical. Scurvy is confirmed with a low vitamin C level. MR findings will resolve with treatment with ascorbic acid.<sup>59</sup>

### Anorexia Nervosa

Anorexia nervosa is a condition that is characterized by an intense fear of gaining weight and a disturbance with one's body image, resulting in restriction in food intake and a low body mass index. Anorexia nervosa has a prevalence rate of 0.3% in young females and there are approximately 8 cases per 100,000 per year.<sup>60</sup> Complications arising from anorexia nervosa affect every organ system, including the musculoskeletal system. Patients with anorexia are at an increased risk of osteoporosis, insufficiency fractures, and skeletal immaturity.

While body fat reserves are depleted in anorexia, the bone marrow fat increases when compared to healthy control subjects, suggesting adipogenesis and premature conversion of red marrow to yellow marrow.<sup>61</sup> Marrow fat correlates inversely to bone mineral density, leading to early osteoporosis and increased risk of insufficiency fractures.<sup>38,61</sup> MR findings of the bone marrow in patients with anorexia nervosa include increased signal intensity on T1-weighted imaging, reflective of the increased bone marrow fat content. These findings, in combination with the patient's age and demographics should raise suspicion of an underlying eating disorder.<sup>38,61</sup>

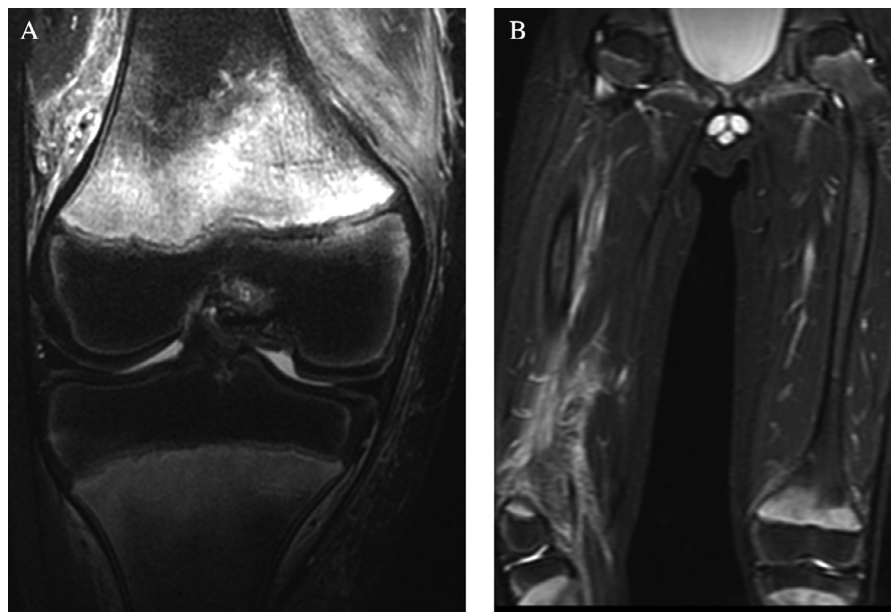


**Figure 20** Scurvy. A 9-year-old boy with knee pain, no fever and normal inflammatory markers. (A) Coronal STIR image of the knee shows distal femoral metaphyseal edema with adjacent soft tissue edema. There is no cortical disruption and marrow signal in the epiphysis is normal. Given the appearance of the knee and clinical scenario, a coronal STIR large field of view was obtained of the femurs which showed symmetric metaphyseal abnormalities involving the distal femurs, proximal tibiae, and proximal femurs. A diagnosis of scurvy was made. The child had undetectable vitamin C levels and was found to have a very restricted diet.

## Infectious and Inflammatory Conditions

### Acute Hematogenous Osteomyelitis

Acute hematogenous osteomyelitis is an infection that primarily affects the most vascularized structures of the growing skeleton. The most common organism is *Staphylococcus aureus*, followed by the respiratory pathogens *Kingella kingae*, *Streptococcus pyogenes*, and *Streptococcus pneumoniae*. Methicillin-resistant *S. aureus* accounts for 30%-40% of osteoarticular infections in the United States.<sup>62</sup> Because of its rich vascularity, the metaphyses and metaphyseal equivalents are the most common sites for osteomyelitis. Transphyseal spread of infection is very common in children<sup>63</sup> and may lead to destruction of the epiphyseal cartilage and secondary ossification center. The inflammation may affect the germinal zone of the physis, leading to permanent growth disturbance.<sup>62</sup>

MR is the modality of choice to evaluate osteomyelitis and includes a combination of T1-weighted and fluid-sensitive sequences. Infection within the bone typically manifests as decreased signal intensity on T1-weighted images with increased signal on fluid-sensitive sequences. After intravenous gadolinium, the affected bone usually shows increased enhancement; however, in areas of infected, ischemic marrow, there may be heterogeneous or diffusely decreased enhancement. Marrow ischemia is thought to be due to increased intramedullary pressure, vascular thrombosis and destruction of the periosteal blood supply.<sup>62</sup> The use of intravenous gadolinium is important to consider when evaluating for soft tissue abscesses, bone or subperiosteal abscesses, associated deep venous thrombosis (particularly in methicillin-resistant *S. aureus* infection) and infectious chondritis in infants and very young children. The presence of these findings may affect surgical management (Fig. 21).<sup>62</sup> Of note, in older children with subperiosteal abscesses, it is not

uncommon to see high signal intensity foci on T1-weighted images. These foci reflect fat globules and are formed by the lytic effect of the bacterial enzymes, resulting in lysis of marrow adipocytes. The presence of these subperiosteal fat globules may help to differentiate osteomyelitis from other processes such as tumor (Fig. 22).<sup>62</sup>

### Chronic Nonbacterial Osteomyelitis

Chronic nonbacterial osteomyelitis (CNO) is an aseptic, autoimmune inflammatory disorder of bone that primarily occurs in children. Patients typically present with bone pain with a relapsing and remitting course.<sup>64</sup> The disease is known by many names and was first described as a symmetric multifocal osteomyelitis, known as chronic recurrent multifocal osteomyelitis. However, because the disease may be unifocal and not relapsing, the umbrella term CNO is more suitable.<sup>65</sup> Clinically, patients with CNO typically present with nonspecific complaints such as bone pain, tenderness, swelling or limited range of motion at one or more sites. Systemic symptoms such as fever and weight loss are usually not present. The duration of symptoms can vary significantly from several days to years due to the insidious onset and vague symptoms. Laboratory results are usually normal with the most common finding being mildly elevated inflammatory markers (sedimentation rate and C-reactive protein). A personal history or family history of autoimmune disease is common.<sup>64</sup>

CNO lesions occur at typical sites: metaphyses of the tubular long bones, medial aspect of the clavicle, spine, pelvis (metaphyseal equivalents), sacroiliac joint, ribs, and mandible. Lower extremity involvement is much more common than the upper extremity.<sup>64</sup> At presentation, 30% of cases will present as unifocal lesions. However, most children will develop multifocal lesions within 4 years. When multifocal

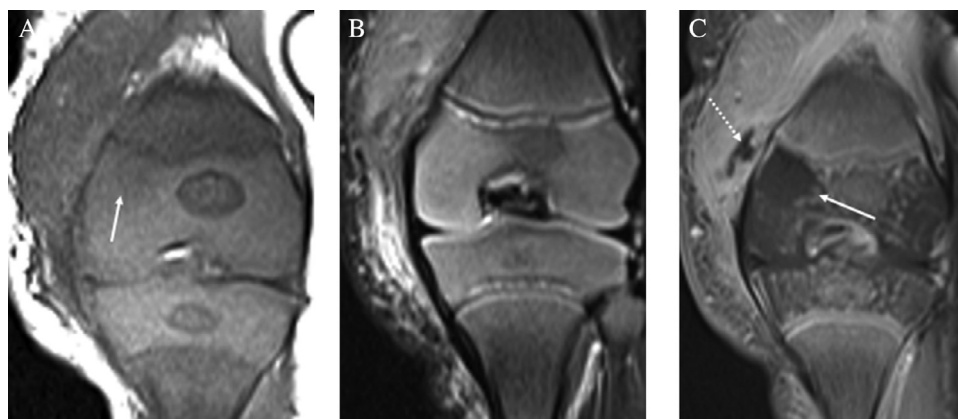


**Figure 21** Infectious chondritis. A 3-week-old boy with abrupt onset of left knee swelling and high fever. (A) Coronal T1-weighted of the knee demonstrates very subtle hypointensity within the medial aspect of the distal femoral epiphysis (arrow). (B) Coronal T2-weighted fat-saturated image shows no focal abnormality within the epiphysis; however, there is a large amount of soft tissue edema seen along the medial aspect of the knee (arrows). (C) Coronal T1-weighted fat-saturated postcontrast image shows nonenhancement of the medial aspect of the distal femoral epiphyses (solid arrow) compatible with infectious chondritis with an adjacent subcutaneous abscess (dashed arrow). The epiphyseal abnormality in this neonate is conspicuous only after the administration of IV gadolinium contrast. Cultures yielded Group A streptococcus.



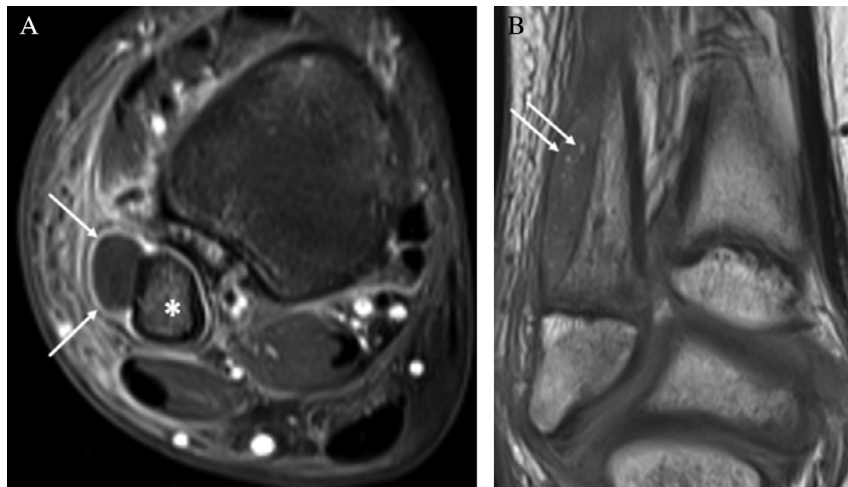


**Figure 22** Acute hematogenous osteomyelitis of the distal fibula. A 10-year-old boy with ankle pain, swelling, and fever. (A) Axial T1-weighted fat-saturated postcontrast image of the ankle demonstrates abnormal enhancement of the distal fibular metaphysis (\*) with a subperiosteal abscess (arrows). (B) Coronal T1-weighted image shows the subperiosteal abscess with numerous hyperintense foci (arrows) compatible with fat globules. These globules are formed by lysis of marrow adipocytes due to bacterial enzymes.

lesions are present, the disease is symmetric in 40% of cases.<sup>65</sup>

Conventional radiography is the typical first line imaging modality, followed by MR. On radiography, most lesions are lytic during the early phase, followed by sclerosis with or without periosteal reaction. MR is useful for determining the extent of disease as well as surveillance. On MR, lesions are hyperintense on fluid-sensitive sequences and hypointense on T1-weighted images (Fig. 23). Lesions may also demonstrate periostitis, osseous remodeling or hyperostosis, soft tissue inflammation and transphyseal disease which may result in growth arrest. Clinically occult joint effusions are present in up to 30% of patients. The presence of a large fluid collection or abscess, fistulous tract or sequestrum makes the diagnosis of bacterial osteomyelitis more likely than CNO.<sup>64</sup> In indeterminate cases, bone biopsy is suggested to exclude

infection or malignancy. Zhao et al<sup>65</sup> recommend that a whole body MR protocol should consist of coronal STIR, sagittal STIR of the entire spine, sagittal STIR feet, and axial STIR of pelvis and knees.

## Marrow Edema Syndrome

Bone marrow edema syndrome comprises several clinical conditions including transient osteoporosis of the hip, regional migratory osteoporosis and complex regional pain syndrome.<sup>66</sup> Of these, only complex regional pain syndrome, specifically the type 1 variant (previously called reflex sympathetic dystrophy), is commonly seen in children.<sup>1</sup> The cause of pediatric complex regional pain syndrome is not well understood but likely represents a dysfunctional neurologic,

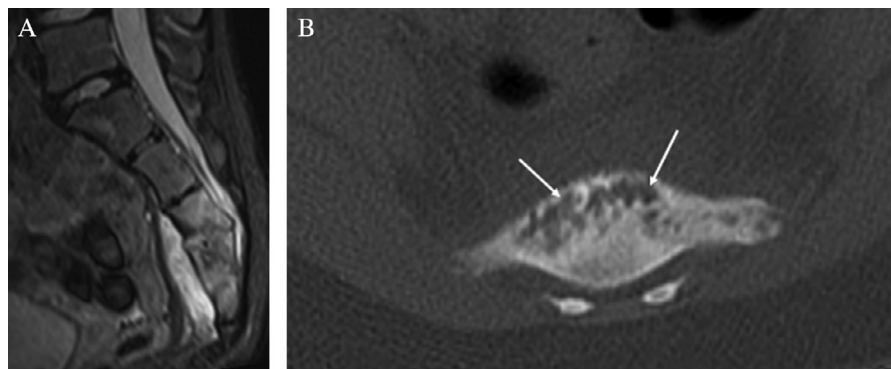


**Figure 23** Chronic nonbacterial osteomyelitis. A 10-year-old girl with lower back pain for 6 months. (A) Sagittal T2-weighted fat-saturated image of the sacrum demonstrates diffuse marrow edema within the mid to distal sacrum with loss of the normal disk space and bone remodeling. The cortex is intact. There is soft tissue edema along the ventral and dorsal aspect of the sacrum. (B) Axial noncontrast CT of S3 obtained during biopsy shows a lytic region within the anterior aspect of the sacrum (arrow) with adjacent sclerosis. There is no cortical destruction or fistulous tract seen. Biopsy showed acute on chronic inflammation.

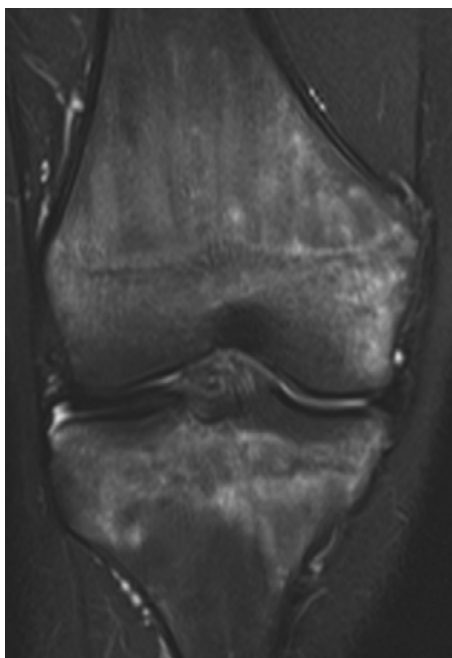


**Figure 24** Bone marrow edema syndrome. A 16-year-old boy with gradually increasing right knee pain over a 10-month period, now unable to bear weight. Coronal T2-weighted fat-saturated image of the knee demonstrates patchy marrow edema within the distal femur and proximal tibia.

inflammatory, or immune response to injury or insult that manifests as hypersensitivity, swelling, atrophy, and stiffness of the affected extremity.<sup>67</sup> Complex regional pain syndrome is more commonly seen in the lower extremities in children, and girls are affected more often than boys.<sup>68</sup> On conventional radiography and CT, complex regional pain syndrome appears as subchondral or subperiosteal osteopenia. MR demonstrates areas of patchy and subcortical bone marrow edema (Fig. 24). There may be evidence of erosive changes to articular surfaces. MR evidence of associated soft tissue trophic changes may be present. Chronically, the marrow imaging appearance of complex regional pain syndrome is difficult to distinguish from disuse osteopenia.<sup>1</sup> The diagnosis of complex regional pain syndrome is clinical and the role of imaging is often limited to the exclusion of other potential etiologies for the patient's condition.

## Conclusion

MR imaging is a very useful modality to evaluate the bone marrow in children, characterize various types of lesions and infiltrative diseases, identify complications, and guide treatment. Many marrow lesions and infiltrative processes have unique features seen on MRI; however, there are similar features among pathologic processes, as well as with normal age-related bone marrow changes that often make diagnosis difficult. Therefore, as a radiologist, it is essential to understand the age-related bone marrow changes and distinguish

them from the various pathologic conditions in order to make an accurate diagnosis.

## References

1. Chan BY, Gill KG, Rebsamen SL, et al: MR imaging of pediatric bone marrow. *Radiographics* 36:1911-1930, 2016. <https://doi.org/10.1148/rg.2016160056>
2. Burdiles A, Babyn PS: Pediatric bone marrow MR imaging. *Magn Reson Imaging Clin N Am* 17:391-409, 2009. <https://doi.org/10.1016/j.mric.2009.03.001>. v.
3. Laor T, Jaramillo D: MR imaging insights into skeletal maturation: What is normal? *Radiology* 250:28-38, 2009. <https://doi.org/10.1148/radiol.2501071322>
4. Sebag GH, Dubois J, Tabet M: Pediatric spinal bone marrow: Assessment of normal age-related changes in the MRI appearance. *Pediatr Radiol* 23:515-518, 1993. <https://doi.org/10.1007/bf02012134>
5. Jaimes C, Chauvin NA, Delgado J, et al: MR imaging of normal epiphyseal development and common epiphyseal disorders. *Radiographics* 34:449-471, 2014. <https://doi.org/10.1148/rg.342135070>
6. Chauvin NA, Jaimes C, Khwaja A: Ankle and foot injuries in the young athlete. *Semin Musculoskelet Radiol* 22:104-117, 2018. <https://doi.org/10.1055/s-0037-1609012>
7. Jaimes C, Jimenez M, Marin D, et al: The trochlear pre-ossification center: A normal developmental stage and potential pitfall on MR images. *Pediatr Radiol* 42:1364-1371, 2012. <https://doi.org/10.1007/s00247-012-2454-7>
8. Zbojnicewicz AM, Laor T: Focal periphyseal edema (FOPE) zone on MRI of the adolescent knee: A potentially painful manifestation of physiologic physeal fusion? *AJR Am J Roentgenol* 197:998-1004, 2011. <https://doi.org/10.2214/AJR.10.6243>
9. Hwang S, Panicek DM: Magnetic resonance imaging of bone marrow in oncology, Part 2. *Skelet Radiol* 36:1017-1027, 2007. <https://doi.org/10.1007/s00256-007-0308-4>
10. Hwang S, Panicek DM: Magnetic resonance imaging of bone marrow in oncology, Part 1. *Skelet Radiol* 36:913-920, 2007. <https://doi.org/10.1007/s00256-007-0309-3>
11. Chavhan GB, Alsabban Z, Babyn PS: Diffusion-weighted imaging in pediatric body MR imaging: Principles, technique, and emerging applications. *Radiographics* 34:E73-E88, 2014. <https://doi.org/10.1148/rg.343135047>
12. Gottumukkala RV, Gee MS, Hampilos PJ, et al: Current and emerging roles of whole-body MRI in evaluation of pediatric cancer patients. *Radiographics* 39:516-534, 2019. <https://doi.org/10.1148/rg.2019180130>
13. Ording Muller LS, Avenarius D, Olsen OE: High signal in bone marrow at diffusion-weighted imaging with body background suppression (DWIBS) in healthy children. *Pediatr Radiol* 41:221-226, 2011. <https://doi.org/10.1007/s00247-010-1774-8>
14. Arkader A, Glotzbecker M, Hosalkar HS, et al: Primary musculoskeletal Langerhans cell histiocytosis in children: An analysis for a 3-decade period. *J Pediatr Orthop* 29:201-207, 2009. <https://doi.org/10.1097/BPO.0b013e3181982aa2>
15. Hayashida Y, Yakushiji T, Awai K, et al: Monitoring therapeutic responses of primary bone tumors by diffusion-weighted image: Initial results. *Eur Radiol* 16:2637-2643, 2006. <https://doi.org/10.1007/s00330-006-0342-y>
16. Goo HW: Whole-body MRI in children: Current imaging techniques and clinical applications. *Korean J Radiol* 16:973-985, 2015. <https://doi.org/10.3348/kjr.2015.16.5.973>
17. Morone M, Bali MA, Tunariu N, et al: Whole-body MRI: Current applications in oncology. *AJR Am J Roentgenol* 209:W336-W349, 2017. <https://doi.org/10.2214/AJR.17.17984>
18. Lindsay AJ, Delgado J, Jaramillo D, et al: Extended field of view magnetic resonance imaging for suspected osteomyelitis in very young children: Is it useful? *Pediatr Radiol* 49:379-386, 2019. <https://doi.org/10.1007/s00247-018-4317-3>

19. Voit AM, Arnoldi AP, Douis H, et al: Whole-body magnetic resonance imaging in chronic recurrent multifocal osteomyelitis: Clinical longterm assessment may underestimate activity. *J Rheumatol* 42:1455-1462, 2015. <https://doi.org/10.3899/jrheum.141026>
20. Anupindi SA, Chauvin NA, Nichols KE: Reply to "Whole-body MRI screening in children with Li-Fraumeni and other cancer-predisposition syndromes". *AJR Am J Roentgenol* 206:W53, 2016. <https://doi.org/10.2214/AJR.15.15646>
21. Rozenfeld MN, Podberesky DJ: Gadolinium-based contrast agents in children. *Pediatr Radiol* 48:1188-1196, 2018. <https://doi.org/10.1007/s00247-018-4165-1>
22. Mirabello L, Troisi RJ, Savage SA: Osteosarcoma incidence and survival rates from 1973 to 2004: Data from the surveillance, epidemiology, and end results program. *Cancer* 115:1531-1543, 2009. <https://doi.org/10.1002/cncr.24121>
23. van den Berg H, Kroon HM, Slaar A, et al: Incidence of biopsy-proven bone tumors in children: A report based on the Dutch pathology registration "PALGA". *J Pediatr Orthoped* 28:29-35, 2008. <https://doi.org/10.1097/BPO.0b013e3181558cb5>
24. Duchman KR, Gao Y, Miller BJ: Prognostic factors for survival in patients with Ewing's sarcoma using the surveillance, epidemiology, and end results (SEER) program database. *Cancer Epidemiol* 39:189-195, 2015. <https://doi.org/10.1016/j.canep.2014.12.012>
25. Weber MA, Papakonstantinou O, Nikodinovska VV, et al: Ewing's sarcoma and primary osseous lymphoma: Spectrum of imaging appearances. *Semin Musculoskelet Radiol* 23:36-57, 2019. <https://doi.org/10.1055/s-0038-1676125>
26. Murphey MD, Senchak LT, Mambalam PK, et al: From the radiologic pathology archives: Ewing sarcoma family of tumors: Radiologic-pathologic correlation. *Radiographics* 33:803-831, 2013. <https://doi.org/10.1148/rg.333135005>
27. Peersman B, Vanhoenacker FM, Heyman S, et al: Ewing's sarcoma: Imaging features. *JBR-BTR* 90:368-376, 2007
28. Demircay E, Hornicek FJ Jr., Mankin HJ, et al: Malignant lymphoma of bone: A review of 119 patients. *Clin Orthop Relat Res* 471:2684-2690, 2013. <https://doi.org/10.1007/s11999-013-2991-x>
29. Chisholm KM, Ohgami RS, Tan B, et al: Primary lymphoma of bone in the pediatric and young adult population. *Hum Pathol* 60:1-10, 2017. <https://doi.org/10.1016/j.humpath.2016.07.028>
30. Krishnan A, Shirkhoda A, Tehranzadeh J, et al: Primary bone lymphoma: Radiographic-MR imaging correlation. *Radiographics* 23:1371-1383, 2003. <https://doi.org/10.1148/rg.236025056> discussion 1384-1377
31. DuBois SG, Kalika Y, Lukens JN, et al: Metastatic sites in stage IV and IVS neuroblastoma correlate with age, tumor biology, and survival. *J Pediatr Hematol Oncol* 21:181-189, 1999. <https://doi.org/10.1097/00043426-199905000-00005>
32. Weiss AR, Lyden ER, Anderson JR, et al: Histologic and clinical characteristics can guide staging evaluations for children and adolescents with rhabdomyosarcoma: A report from the Children's Oncology Group Soft Tissue Sarcoma Committee. *J Clin Oncol* 31:3226-3232, 2013. <https://doi.org/10.1200/JCO.2012.44.6476>
33. Guyot-Goubin A, Donadieu J, Barkaoui M, et al: Descriptive epidemiology of childhood Langerhans cell histiocytosis in France, 2000-2004. *Pediatr Blood Cancer* 51:71-75, 2008. <https://doi.org/10.1002/pbc.21498>
34. Zaveri J, La Q, Yarmish G, et al: More than just Langerhans cell histiocytosis: A radiologic review of histiocytic disorders. *Radiographics* 34:2008-2024, 2014. <https://doi.org/10.1148/rg.347130132>
35. Samet J, Weinstein J, Fayad LM: MRI and clinical features of Langerhans cell histiocytosis (LCH) in the pelvis and extremities: Can LCH really look like anything? *Skelet Radiol* 45:607-613, 2016. <https://doi.org/10.1007/s00256-016-2330-x>
36. Kellenberger CJ: Pitfalls in paediatric musculoskeletal imaging. *Pediatr Radiol* 39(suppl 3):372-381, 2009. <https://doi.org/10.1007/s00247-009-1220-y>
37. Goo HW, Yang DH, Ra YS, et al: Whole-body MRI of Langerhans cell histiocytosis: Comparison with radiography and bone scintigraphy. *Pediatr Radiol* 36:1019-1031, 2006. <https://doi.org/10.1007/s00247-006-0246-7>
38. Bredella MA, Fazeli PK, Miller KK, et al: Increased bone marrow fat in anorexia nervosa. *J Clin Endocrinol Metab* 94:2129-2136, 2009. <https://doi.org/10.1210/jc.2008-2532>
39. Tang YM, Jeavons S, Stuckey S, et al: MRI features of bone marrow necrosis. *AJR Am J Roentgenol* 188:509-514, 2007. <https://doi.org/10.2214/AJR.05.0656>
40. Saini A, Saifuddin A: MRI of osteonecrosis. *Clin Radiol* 59:1079-1093, 2004. <https://doi.org/10.1016/j.crad.2004.04.014>
41. Hanrahan CJ, Shah LM: MRI of spinal bone marrow: Part 2, T1-weighted imaging-based differential diagnosis. *AJR Am J Roentgenol* 197:1309-1321, 2011. <https://doi.org/10.2214/AJR.11.7420>
42. Stevens SK, Moore SG, Kaplan ID: Early and late bone-marrow changes after irradiation: MR evaluation. *AJR Am J Roentgenol* 154:745-750, 1990. <https://doi.org/10.2214/ajr.154.4.2107669>
43. Daldrop-Link HE, Henning T, Link TM: MR imaging of therapy-induced changes of bone marrow. *Eur Radiol* 17:743-761, 2007. <https://doi.org/10.1007/s00330-006-0404-1>
44. Sacks EL, Goris ML, Glatstein E, et al: Bone marrow regeneration following large field radiation: Influence of volume, age, dose, and time. *Cancer* 42:1057-1065, 1978. [https://doi.org/10.1002/1097-0142\(197809\)42:3<1057::aid-cncr2820420304>3.0.co;2-p](https://doi.org/10.1002/1097-0142(197809)42:3<1057::aid-cncr2820420304>3.0.co;2-p)
45. Roebuck DJ: Skeletal complications in pediatric oncology patients. *Radiographics* 19:873-885, 1999. <https://doi.org/10.1148/radiographics.19.4.g99jl01873>
46. Mostoufi-Moab S, Isaacoff EJ, Spiegel D, et al: Childhood cancer survivors exposed to total body irradiation are at significant risk for slipped capital femoral epiphysis during recombinant growth hormone therapy. *Pediatr Blood Cancer* 60:1766-1771, 2013. <https://doi.org/10.1002/pbc.24667>
47. Fletcher BD, Wall JE, Hanna SL: Effect of hematopoietic growth factors on MR images of bone marrow in children undergoing chemotherapy. *Radiology* 189:745-751, 1993. <https://doi.org/10.1148/radiology.189.3.7694312>
48. Wang M: Iron deficiency and other types of anemia in infants and children. *Am Fam Physician* 93:270-278, 2016
49. Galanello R, Origa R: Beta-thalassemia. *Orphanet J Rare Dis* 5:11, 2010. <https://doi.org/10.1186/1750-1172-5-11>
50. McCavit TL: Sickle cell disease. *Pediatr Rev* 33:195-204, 2012. <https://doi.org/10.1542/pir.33-5-195> quiz 205-196
51. Ejindu VC, Hine AL, Mashayekhi M, et al: Musculoskeletal manifestations of sickle cell disease. *Radiographics* 27:1005-1021, 2007. <https://doi.org/10.1148/rg.274065142>
52. Guillerman RP: Marrow: Red, yellow and bad. *Pediatr Radiol* 43(suppl 1):S181-S192, 2013. <https://doi.org/10.1007/s00247-012-2582-0>
53. Malkiewicz A, Dziedzic M: Bone marrow reconversion—Imaging of physiological changes in bone marrow. *Pol J Radiol* 77(4):45-50, 2012
54. Lonergan GJ, Cline DB, Abbondanzo SL: Sickle cell anemia. *Radiographics* 21:971-994, 2001. <https://doi.org/10.1148/radiographics.21.4.g01jl23971>
55. Guermazi A, de Kerviler E, Cazals-Hatem D, et al: Imaging findings in patients with myelofibrosis. *Eur Radiol* 9:1366-1375, 1999. <https://doi.org/10.1007/s003300050850>
56. Naithani R, Tyagi S, Choudhry VP: Secondary myelofibrosis in children. *J Pediatr Hematol Oncol* 30:196-198, 2008. <https://doi.org/10.1097/MPH.0b013e318161a9b8>
57. Gongidi P, Johnson C, Dinan D: Scurvy in an autistic child: MRI findings. *Pediatr Radiol* 43:1396-1399, 2013. <https://doi.org/10.1007/s00247-013-2688-z>
58. Choi SW, Park SW, Kwon YS, et al: MR imaging in a child with scurvy: A case report. *Korean J Radiol* 8:443-447, 2007. <https://doi.org/10.3348/kjr.2007.8.5.443>
59. Karthiga S, Dubey S, Garber S, et al: Scurvy: MRI appearances. *Rheumatology (Oxford)* 47:1109, 2008. <https://doi.org/10.1093/rheumatology/ken160>
60. Hoek HW, van Hoeken D: Review of the prevalence and incidence of eating disorders. *Int J Eat Disord* 34:383-396, 2003. <https://doi.org/10.1002/eat.10222>

61. Ecklund K, Vajapeyam S, Feldman HA, et al: Bone marrow changes in adolescent girls with anorexia nervosa. *J Bone Miner Res* 25:298-304, 2010. <https://doi.org/10.1359/jbmr.090805>
62. Jaramillo D, Dormans JP, Delgado J, et al: Hematogenous osteomyelitis in infants and children: Imaging of a changing disease. *Radiology* 283:629-643, 2017. <https://doi.org/10.1148/radiol.2017151929>
63. Gilbertson-Dahdal D, Wright JE, Krupinski E, et al: Transphyseal involvement of pyogenic osteomyelitis is considerably more common than classically taught. *AJR Am J Roentgenol* 203:190-195, 2014. <https://doi.org/10.2214/AJR.13.11279>
64. Khanna G, Sato TS, Ferguson P: Imaging of chronic recurrent multifocal osteomyelitis. *Radiographics* 29:1159-1177, 2009. <https://doi.org/10.1148/rg.294085244>
65. Zhao Y, Ferguson PJ: Chronic nonbacterial osteomyelitis and chronic recurrent multifocal osteomyelitis in children. *Pediatr Clin North Am* 65:783-800, 2018. <https://doi.org/10.1016/j.pcl.2018.04.003>
66. Korompilias AV, Karantanas AH, Lykissas MG, et al: Bone marrow edema syndrome. *Skelet Radiol* 38:425-436, 2009. <https://doi.org/10.1007/s00256-008-0529-1>
67. Weissmann R, Uziel Y: Pediatric complex regional pain syndrome: A review. *Pediatr Rheumatol Online J* 14:29, 2016. <https://doi.org/10.1186/s12969-016-0090-8>
68. Low AK, Ward K, Wines AP: Pediatric complex regional pain syndrome. *J Pediatr Orthop* 27:567-572, 2007. <https://doi.org/10.1097/BPO.0b013e318070cc4d>